10.2478/msr-2013-0030

Portable Light Pen 3D Vision Coordinate Measuring System-Probe Tip Center Calibration

Shugui Liu, Hongling Zhang, Yinghua Dong, Shaliang Tang, Zhenzhu Jiang

State Key Laboratory of Precision Measuring Technology and Instruments, Tianjin University, Tianjin, 300072, China, zhanghl@tju.edu.cn

For different tasks, probe tip should be changed in the 3D vision coordinate measuring system and the accurate determination of probe tip center position is critical. A novel and simple approach for calibrating the probe tip center position of the light pen is presented in this paper. Hundreds of images of the light pen with different postures are collected while the probe tip is kept in firm contact with a reference conical hole. The probe tip position is determined by computing the rotation matrix and translation vector from the obtained images by using the least square fitting method. The experimental results demonstrate the effectiveness of the proposed approach. Its repeatability reaches 0.033 mm, 0.030 mm, and 0.043 mm in *x*, *y*, and *z* axes, respectively, and its convergence speed is satisfactory.

Keywords: Probe tip, center calibration, light pen, portable 3D vision coordinate measuring system, reference conical hole

1. INTRODUCTION

3D POSITIONING and coordinate measuring are the key techniques in manufacturing, reverse engineering of automobile, aviation and many other industries. As a kind of mature product, 3D coordinate measuring machines (CMMs) have gained widespread acceptance for the advantages of wide measuring range, high accuracy, etc. [1]. However, their measuring range and flexibility are limited and can hardly meet the needs of large-scale engineering metrology on the spot.

In recent years, most researches focused on fast and portable measuring techniques for large-scale workpieces [2]. Portable 3D vision coordinate measurement machines (PCMMs) bring great convenience to complete the rapid measurement task in situ due to their portability and have been widely applied in large-scale engineering metrology. There are two main types of measuring techniques: non-contact and contact ones. Representative non-contact PCMMs are laser or white light scanners [3], [4] and laser tracking systems (LTS) with CCD (Charge Coupled Device) cameras [5]-[9]. They often use interferometry or laser triangulation metrology to detect the surface form of the object or track the robot motion. However, a large number of feature points should be sampled on the surface of the object discretely while measuring the profile and it is a time-consuming work when the object is large. In addition, non-contact systems cannot measure the form of hidden features such as deep holes.

PCMMs with light pen are a kind of newly developed contact machines since the 90's. A large number of commercially available systems such as T-Probe, Solo/duo and Actiris have been put into market by Lecia, Metronor and Acticm, respectively [10]. In China, S.G. Liu and F.S. Huang et al. (2005) firstly proposed a light pen 3D vision coordinate measuring system with single CCD camera [11]. Later, many other scholars studied light pen PCMMs with both single CCD camera and binocular stereo vision [12]-[14] and acquired some achievements. All these systems measure the features in non-Cartesian coordinate systems and own the advantages of light weight and flexibility. In PVCMM only the images of control points on the light pen, not the image of the probe tip, need to be captured for determining the coordinates of the points being measured. Moreover, the probe tips should be changed appropriately to complete the measuring process under certain circumstances, especially for measuring large-scale workpieces with small holes, invisible points or corners.

For the PVCMM with light pen, accurate determination of probe tip center position is critical for obtaining correct measured results. The tip center position is asked to be calibrated in real time. The location of the probe tip center might be different when the same probe is installed with different forces. In the past, the position of probe tip was estimated in accordance with the design of the light pen and the true center position might have been different from the estimated one.

In order to improve the measurement accuracy, a novel and fast approach based on [11] to calibrate the center position of the probe tip in situ is proposed in this paper. In section 2, the portable 3D vision coordinate measuring system with an improved light pen is introduced. In section 3, the calibration model of the probe tip center is established and solved. In section 4, a set of experiments are conducted to attest the validity and practicability of the proposed method.

2. PORTABLE LIGHT PEN 3D VISION COORDINATE MEASURING SYSTEM

Fig.1.(a) shows the configuration of the portable light pen 3D vision coordinate measuring system which consists of three parts: a CCD camera, a computer and a light pen. The object being measured in Fig.1. might be the workpiece under measurement or a reference cone used for probe tip calibration. A detailed description of the measuring system is given in [11]. As an improvement, the light pen has been changed in design and takes the form of a rod with ten round LED targets as shown in Fig.1.(b). The first four targets are located in a line on the back plane and the other six on the front plane with two ranks parallel to the back one.

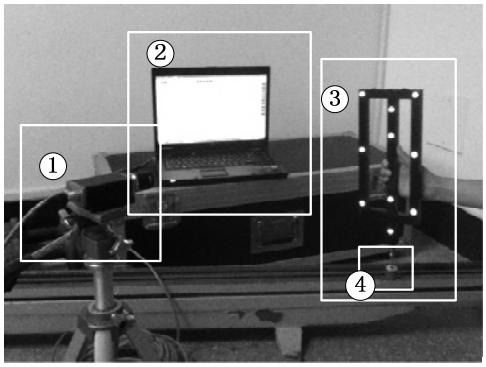

(a) System configuration

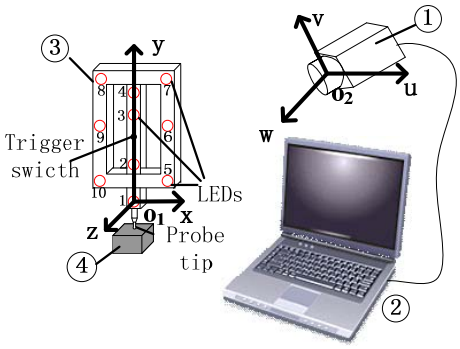

(b) Coordinate system establishment

Fig.1. Portable 3D vision coordinate measuring system (① CCD camera, ② computer, ③ light pen, ④ object being measured).

The diameter of each target is 1cm. However, their center position deviations are inevitable due to manufacturing errors of the light pen and the targets deviate from their nominal positions. The accurate center coordinates of these ten LED targets (x_j, y_j, z_j), $j = 1,2,\cdots 10$ in the light pen coordinate system should be calibrated by an image measuring apparatus [15].

Three coordinate systems are established as shown in Fig.1.(b), and they are defined as follows.

(a) Light pen coordinate system $o_1 - xyz$ with origin at the projection of the center of the first target on the front plane, in which the projection of the line connecting the first and fourth LEDs on the front plane is assigned as the *y*-axis, and the line perpendicular to *y*-axis on the front plane is defined as *x*-axis. The other six LEDs are on the plane of o_1xy . *z*-axis is determined according to the right-handed rule. The light pen coordinate system is established when measuring the center positions of LED light target using the image measuring apparatus.

(b) Camera coordinate system $o_2 - uvw$ with origin at the perspective center of the camera, in which *u* and *v* axes are in the horizontal and vertical directions, respectively. The axis from the perspective center o_2 pointing to the intersection point of the optical axis and the image plane is defined as the *w* axis.

(c) Image plane coordinate system $O - XY$ with origin at the image plane center, in which *X* and *Y* axes are parallel to the horizontal and vertical scanning directions of the CCD camera, respectively.

The relationship between $o_2 - uvw$ and $o_1 - xyz$ can be described by rotation matrix R and translation vector T:

$$\begin{bmatrix} u \\ v \\ w \end{bmatrix} = \begin{bmatrix} R & T \end{bmatrix} \begin{bmatrix} x \\ y \\ z \\ 1 \end{bmatrix} = \begin{bmatrix} r_1 & r_2 & r_3 & t_x \\ r_4 & r_5 & r_6 & t_y \\ r_7 & r_8 & r_9 & t_z \end{bmatrix} \begin{bmatrix} x \\ y \\ z \\ 1 \end{bmatrix} \quad (1)$$

where $R = \begin{bmatrix} r_1 & r_2 & r_3 \\ r_4 & r_5 & r_6 \\ r_7 & r_8 & r_9 \end{bmatrix}$, $T = \begin{bmatrix} t_x \\ t_y \\ t_z \end{bmatrix}$.

When measuring, the image of the light pen with ten alight LED targets is captured by the CCD camera which has been pre-calibrated [16], [17] and transferred to the computer through a gigabit network cable. The software installed in the computer processes the image to obtain the center positions of targets (X_{uj}, Y_{uj}), $j = 1,2,\cdots 10$ on the image plane [18]. Then these ten pairs of center coordinates are used as the inputs to calculate rotation matrix R and translation vector T . Before measuring, the center position of the probe tip in the light pen coordinate system (x_0, y_0, z_0) should be calibrated in advance. So the coordinates of the probe tip center in the camera coordinate system, which corresponds to the position of the point under measurement, can be acquired from (1).

3. PROBE TIP CENTER POSITION CALIBRATION

A. Establishment of the calibration model

The probe tip is brought into contact with the reference cone which is fixed on a vibration isolated table in front of the CCD camera of the portable 3D vision coordinate measuring system. Fix the CCD camera on the vibration isolated table and adjust its position to ensure that all ten control points (LED targets) of the light pen appear fully in the view field when the rotation range of the light pen is proper. Swing the light pen with ten alight LEDs smoothly while keeping the probe tip in firm contact with the reference cone hole as shown in Fig.2. Images with different postures of the light pen are taken by the CCD camera and transferred to the computer.

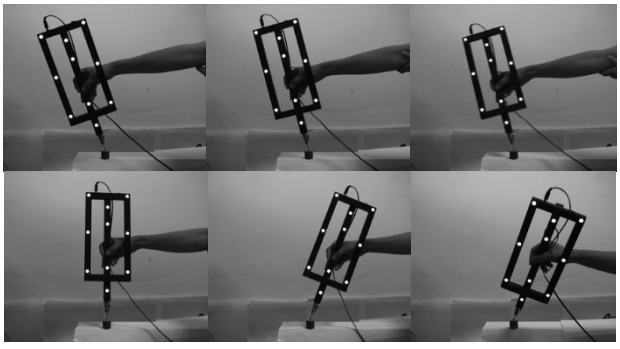

Fig.2. Image collection in several postures.

Suppose the ideal coordinates of the probe tip center in o_1-xyz and o_2-uvw are $(x_0, y_0, z_0)^{\mathrm{T}}$ and $(u_0, v_0, w_0)^{\mathrm{T}}$, respectively. As the light pen is in firm contact with the reference cone hole, $(x_0, y_0, z_0)^{\mathrm{T}}$ can be thought to be constants. Since the relative position of the CCD camera with reference to the cone hole does not change, $(u_0, v_0, w_0)^{\mathrm{T}}$ can also be considered as constants.

For image i, the measured coordinates of the probe tip center in o_2-uvw are $(u_i, v_i, w_i)^{\mathrm{T}}$, and the following equation can be written:

$$\begin{bmatrix} u_i \\ v_i \\ w_i \end{bmatrix} = \begin{bmatrix} r_{1i} & r_{2i} & r_{3i} & t_{xi} \\ r_{4i} & r_{5i} & r_{6i} & t_{yi} \\ r_{7i} & r_{8i} & r_{9i} & t_{zi} \end{bmatrix} \begin{bmatrix} x_0 \\ y_0 \\ z_0 \\ 1 \end{bmatrix} = \begin{bmatrix} r_{1i}x_0 + r_{2i}y_0 + r_{3i}z_0 + t_{xi} \\ r_{4i}x_0 + r_{5i}y_0 + r_{6i}z_0 + t_{yi} \\ r_{7i}x_0 + r_{8i}y_0 + r_{9i}z_0 + t_{zi} \end{bmatrix} \quad (2)$$

where $R_i = \begin{bmatrix} r_{1i} & r_{2i} & r_{3i} \\ r_{4i} & r_{5i} & r_{6i} \\ r_{7i} & r_{8i} & r_{9i} \end{bmatrix}$ and $T_i = \begin{bmatrix} t_{xi} \\ t_{yi} \\ t_{zi} \end{bmatrix}$ can be acquired

from the center coordinates of these ten control points (x_j, y_j, z_j) and their corresponding coordinates on image plane (X_{uj}, Y_{uj}), where $j = 1, 2, \cdots, 10$.

From (2), the deviation of the measured coordinates of the probe tip center in o_2-uvw from the ideal ones can be estimated as:

$$f_i(x_0, y_0, z_0, u_0, v_0, w_0) = \sqrt{(u_i - u_0)^2 + (v_i - v_0)^2 + (w_i - w_0)^2} \quad (3)$$

Based on the least square method, the objective function of the optimized solution can be written as:

$$g(X) = \min\{\sum_{i=1}^{n} (f_i)^2\} \quad (4)$$

where the optimized solution X represents $(x_0, y_0, z_0, u_0, v_0, w_0)$.

B. Two stages for solving parameters $(x_0, y_0, z_0, u_0, v_0, w_0)$

Stage 1: Computation of R_i and T_i for image i

As mentioned above, (X_{uj}, Y_{uj}) and (x_j, y_j, z_j), $j = 1, 2, \cdots, 10$ are the center coordinates of ten control points on the image plane and those in the light pen coordinate system, respectively. (X_{uj}, Y_{uj}) can be acquired by image processing and (x_j, y_j, z_j) have been measured in advance by an image measuring apparatus.

Based on the camera perspective model [19], for each image:

$$s_j \cdot \begin{bmatrix} X_{uj} \\ Y_{uj} \\ 1 \end{bmatrix} = \begin{bmatrix} f & 0 & 0 \\ 0 & f & 0 \\ 0 & 0 & 1 \end{bmatrix} \begin{bmatrix} r_1 & r_2 & r_3 & t_x \\ r_4 & r_5 & r_6 & t_y \\ r_7 & r_8 & r_9 & t_z \end{bmatrix} \begin{bmatrix} x_j \\ y_j \\ z_j \\ 1 \end{bmatrix} = \begin{bmatrix} fr_1 & fr_2 & fr_3 & ft_x \\ fr_4 & fr_5 & fr_6 & ft_y \\ r_7 & r_8 & r_9 & t_z \end{bmatrix} \begin{bmatrix} x_j \\ y_j \\ z_j \\ 1 \end{bmatrix} \quad (5)$$

where f is the calibrated focal length of the CCD camera.

Let $\begin{bmatrix} fr_1 & fr_2 & fr_3 & ft_x \\ fr_4 & fr_5 & fr_6 & ft_y \\ r_7 & r_8 & r_9 & t_z \end{bmatrix} = t_z \cdot \begin{bmatrix} a_1 & a_2 & a_3 & a_4 \\ a_5 & a_6 & a_7 & a_8 \\ a_9 & a_{10} & a_{11} & 1 \end{bmatrix}$,

$$s_j = r_7 x_j + r_8 y_j + r_9 z_j + t_z = t_z(a_9 x_j + a_{10} y_j + a_{11} z_j + 1) = t_z \zeta_j$$

So (5) can be presented as:

$$\zeta_j \cdot \begin{bmatrix} X_{uj} \\ Y_{uj} \\ 1 \end{bmatrix} == \begin{bmatrix} a_1 & a_2 & a_3 & a_4 \\ a_5 & a_6 & a_7 & a_8 \\ a_9 & a_{10} & a_{11} & 1 \end{bmatrix} \cdot \begin{bmatrix} x_j \\ y_j \\ z_j \\ 1 \end{bmatrix} \quad (6)$$

There are eleven variables in (6). However, they are not totally independent. Rotation matrix R is orthogonal and:

$$\begin{cases} r_1^2 + r_2^2 + r_3^2 = 1 \\ r_4^2 + r_5^2 + r_6^2 = 1 \\ r_7^2 + r_8^2 + r_9^2 = 1 \\ r_1 r_4 + r_2 r_5 + r_3 r_6 = 0 \\ r_1 r_7 + r_2 r_8 + r_3 r_9 = 0 \\ r_7 r_4 + r_8 r_5 + r_9 r_6 = 0 \end{cases} \quad (7)$$

So the optimal solution can be obtained by using Gauss-Newton iteration method [20]. When a_i, i=1,2,…,11 have been determined from (6) and (7), all the components of R and T can be calculated from:

$$\begin{bmatrix} r_1 & r_2 & r_3 & t_x \\ r_4 & r_5 & r_6 & t_y \\ r_7 & r_8 & r_9 & t_z \end{bmatrix} = \begin{bmatrix} \frac{a_1 t_z}{f} & \frac{a_2 t_z}{f} & \frac{a_3 t_z}{f} & \frac{a_4 t_z}{f} \\ \frac{a_5 t_z}{f} & \frac{a_6 t_z}{f} & \frac{a_7 t_z}{f} & \frac{a_8 t_z}{f} \\ a_9 t_z & a_{10} t_z & a_{11} t_z & \frac{1}{\sqrt{a_9^2 + a_{10}^2 + a_{11}^2}} \end{bmatrix} \quad (8)$$

According to (2), $(u_i, v_i, w_i)^{\mathrm{T}}$ can be deduced from the values of R_i and T_i for image i and then the objective function can be expressed by (4) with n images.

Stage 2: Optimization of the objective function

To deal with (4), the general inverse method for the least square solution of nonlinear multivariable equations is employed.

Assume that the system of nonlinear equations is:

$$f_i\left(x_0, y_0, z_0, u_0, v_0, w_0\right) = 0 \quad i = 1, 2, \cdots, n \tag{9}$$

Then the Jacobi matrix of the system of nonlinear equations is presented by:

$$A = \begin{pmatrix} \frac{\partial f_1}{\partial x_0} & \frac{\partial f_1}{\partial y_0} & \frac{\partial f_1}{\partial z_0} & \frac{\partial f_1}{\partial u_0} & \frac{\partial f_1}{\partial v_0} & \frac{\partial f_1}{\partial w_0} \\ \frac{\partial f_2}{\partial x_0} & \frac{\partial f_2}{\partial y_0} & \frac{\partial f_2}{\partial z_0} & \frac{\partial f_2}{\partial u_0} & \frac{\partial f_2}{\partial v_0} & \frac{\partial f_2}{\partial w_0} \\ \vdots & \vdots & \vdots & \vdots & \vdots & \vdots \\ \frac{\partial f_n}{\partial x_0} & \frac{\partial f_n}{\partial y_0} & \frac{\partial f_n}{\partial z_0} & \frac{\partial f_n}{\partial u_0} & \frac{\partial f_n}{\partial v_0} & \frac{\partial f_n}{\partial w_0} \end{pmatrix} \tag{10}$$

The iterative formula for the least square solution to the system of nonlinear equations can be written as:

$$X^{(k+1)} = X^{(k)} - \alpha_k \Delta X^{(k)} \tag{11}$$

where $\Delta X^{(k)}$ is the least square solution to the linear equation set $A^{(k)}\Delta X^{(k)} = F^{(k)}$. $A^{(k)}$ is the Jacobi matrix of $X^{(k)}$; $F^{(k)}$ is the left-side value of the function after *k*-th iteration and can be presented as follows:

$$F^{(k)} = (f_1^{(k)}, f_2^{(k)}, \cdots, f_n^{(k)})^T \tag{12}$$
$$f_i^{(k)} = f_i(x^{(k)}, y^{(k)}, z^{(k)}, u^{(k)}, v^{(k)}, w^{(k)}) \qquad i = 1, 2, \cdots, n$$

where α_k is the value which enables function $\sum_{i=1}^{n} (f_i^{(k+1)})^2$ reaching its minimum value.

Proper initial parameters would reduce the iteration time to a great extent. Six equations can be obtained from two images based on (2). In order to make the initial parameters more proper, six images are used to form over determined linear equations, and their solutions are set as initial parameters of the iterative algorithm. Dozens, even hundreds of images are used to optimize the objective function.

C. Calibration steps

1) Capture images and compute the corresponding matrices R_i and T_i.
2) Calculate the six initial values of the optimized solution X and set $k = 0$.
3) Find the optimal solution of $f_i\left(x_0, y_0, z_0, u_0, v_0, w_0\right) = 0$, $i = 1, 2, \cdots, n$ by using the general inverse method for least square solution.
4) Estimate the convergence based on the increment of $|\alpha_k \Delta X^{(k)}|$. End the iterative calculation when the increment of $|\alpha_k \Delta X^{(k)}|$ is small enough. Otherwise, let $k = k + 1$ and go back to step 3.
5) The position $(x_0, y_0, z_0)^T$ obtained after step 4 is the probe tip position in the light pen coordinate system $o_1 - xyz$.

4. Experiments & Results

A. Repeatability test of the probe tip calibration

The same probe tip is calibrated ten times under different orientations. The test results and their average values (Ave) as well as standard deviations (Std) are shown in Table 1.

Table 1. Center coordinates of the probe tip (mm).

No. of test	*x*-axis	*y*-axis	*z*-axis
1	-1.278	-90.429	-23.903
2	-1.329	-90.388	-23.754
3	-1.339	-90.401	-23.842
4	-1.304	-90.456	-23.844
5	-1.344	-90.397	-23.830
6	-1.353	-90.450	-23.887
7	-1.251	-90.431	-23.855
8	-1.343	-90.388	-23.866
9	-1.311	-90.383	-23.890
10	-1.330	-90.372	-23.877
Ave	-1.3182	-90.4095	-23.8548
Std	0.033	0.030	0.043

Table 2. Coordinates of a fixed point based on different data (mm).

No.	Based on calibrated data			Based on nominal data		
	u-axis	*v*-axis	*w*-axis	*u*-axis	*v*-axis	*w*-axis
1	-4.879	214.298	1087.453	-5.655	214.106	1086.940
2	-4.874	214.294	1087.448	-5.767	214.314	1088.147
3	-4.862	214.284	1087.437	-5.624	214.108	1088.262
4	-4.870	214.291	1087.436	-5.808	214.383	1088.514
5	-4.864	214.281	1087.427	-5.563	214.040	1087.324
6	-4.865	214.289	1087.477	-5.633	214.190	1087.560
7	-4.866	214.278	1087.456	-5.749	214.374	1088.365
8	-4.872	214.289	1087.490	-5.601	214.105	1088.556
9	-4.881	214.285	1087.459	-5.619	214.113	1087.020
10	-4.880	214.279	1087.418	-5.580	214.056	1087.442
Ave	-4.871	214.287	1087.450	-5.660	214.179	1087.813
Std	0.007	0.007	0.022	0.085	0.130	0.623

Close to 300 images are collected in every calibration process and satisfactory convergence values are obtained with the method mentioned above. The test results show that the repeatability of probe tip center position reaches 0.033 mm, 0.030 mm, and 0.043 mm in *x*, *y*, and *z* axes, respectively.

B. Measurement test with the reference cone

A reference cone is used as an assistive tool when calibrating the probe tip. Based on the result produced in the first experiment, the position of the center hole on the reference cone in the camera system $o_2 - uvw$ is measured ten times to test the correctness of the calibration algorithm. As a contrast test, the nominal center coordinates of the probe tip $(0, -90, -25)$ assigned in the design are used to measure the position of the center hole as well. Table 2. shows the results of these two tests.

Obviously, the stability of the coordinates of the fixed point obtained based on calibrated data is much more superior to that based on nominal data. The maximum differences in *u*, *v*, and *w* axes are $(0.019, 0.020, 0.072)$ based on the calibrated data and $(0.245, 0.343, 1.616)$ based on the nominal data.

Table 3. A comparison between measured and actual radii (mm).

No. of test	1	2	3	4	5	6	7	8	Average
Computed value	31.763	31.773	31.776	31.767	31.757	31.758	31.772	31.776	31.768
Absolute error	0.012	0.022	0.025	0.016	0.006	0.007	0.021	0.025	0.017
Relative error ($\times 10^{-4}$)	3.8	6.9	7.9	5.0	1.9	2.2	6.6	7.9	5.4

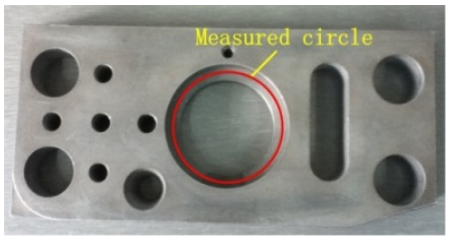

Fig.3. Workpiece used in experiments

C. Measurement test of the system

An experiment on measuring a given circle is performed to testify both the probe tip calibration accuracy and the accuracy of the whole measuring system.

The red circle in the middle of the workpiece shown in Fig.3. is measured eight times by using the mentioned portable 3D vision coordinate measuring system. In each run, 20 points are detected to evaluate the circle. Its radius measured by an orthogonal CMM equal to 31.751 mm is taken as the actual value in our test. The same points are used to calculate the radius in each run. The measured results are shown in Table 3.

It can be seen that the standard deviation of measured radii is 0.008 mm and the difference between the measured average value and the accurate value is 0.017 mm. This satisfactory result proves the validity of the calibration method of the probe tip.

Since the environment factors such as the influence of light and vibration cannot be neglected, the overall accuracy of our portable 3D vision coordinate measuring system is affected to a certain degree.

5. CONCLUSION

In this paper, the mathematical model for calibrating the probe tip center position of the portable 3D vision coordinate measuring system is presented. A reference cone is used to assist this calibration process. The algorithm and procedures for solving the mathematical model are described in detail and validated by three experiments. The first experiment shows that the repeatability errors of probe tip center calibration in *x*, *y*, and *z* axes are 0.033 mm, 0.030 mm, and 0.043, respectively. The other two experiments deal with the mentioned portable 3D vision coordinate measuring system. Based on the calibrated center position of the probe tip, the coordinate stabilities of a fixed point in *u*, *v*, and *w* axes are 0.019 mm, 0.020 mm, and 0.072 mm, respectively. It shows great enhancement in comparison with those based on the nominal center position of the probe tip. The last experiment proves the validity of our calibration method as well as the whole system.

The experiments show that the proposed measuring system can be applied in industry with its obvious advantages of convenience and flexibility in use, high speed and satisfactory accuracy in most cases.

Factors which affect the calibration accuracy and repeatability are discussed. Since the position accuracy of probe tip center is the key factor to guarantee the accuracy of the whole measuring system, so more work on improving the camera calibration accuracy and enhancing the image processing technology should be done in the future.

APPENDIX

1. Variables used in the matrices

(u, v, w)	Coordinates in camera coordinate system $o_2 - uvw$
(x, y, z)	Coordinates in light pen coordinate system $o_1 - xyz$
$(u_0, v_0, w_{0)}$	Nominal coordinates of the probe tip center in camera coordinate system $o_2 - uvw$
(x_0, y_0, z_0)	Nominal coordinates of the probe tip center in light pen coordinate system $o_1 - xyz$
R	Rotation matrix from $o_1 - xyz$ to $o_2 - uvw$
T	Translation vector from $o_1 - xyz$ to $o_2 - uvw$
(u_i, v_i, w_i)	measured coordinates of the probe tip center from image i in $o_2 - uvw$
R_i	Rotation matrix of image i
T_i	Translation vector of image i
f	Focal length of the CCD camera.
(x_j, y_j, z_j)	Center coordinates of ten control points in light pen coordinate system $o_1 - xyz$
(X_{uj},Y_{uj})	Center coordinates of ten control points in image plane coordinate system O-XY

REFERENCES

[1] Bosch, J.A. (1995). *Coordinate Measuring Machines and Systems*. New York: Marcel Dekker Inc., 15-42.

[2] Estler, W.T., Edmundson, K.L., Peggs, G.N., Parker, D.H. (2002). Large-scale metrology - an update. *CIRP Annals - Manufacturing Technology*, 51 (2), 587–609.

[3] Milroy, M.J., Weir, D.J., Bradley, C., Vickers, G.W. (1996). Reverse engineering employing a 3D laser scanner: A case study. *International Journal of Advanced Manufacturing Technology*, 12 (2), 111-121.

[4] Chen, J., Wu, X.J., Wang, M.Y., Li, X.F. (2012). 3D shape modeling using a self-developed hand-held 3D laser scanner and an efficient HT-ICP point cloud registration algorithm. *Optics & Laser Technology*, 46, 414-423.

[5] Vincze, M., Prenninger, J.P., Gander, H. (1994). A laser tracking system to measure position and orientation of robot end effectors under motion. *International Journal of Robotics Research*, 13 (4), 305-314.

[6] Mayer, J.R.R., Parker, G.A. (1994). A portable instrument for 3-D dynamic robot measurements using triangulation and laser tracking. *IEEE Transactions on Robotics and Automation*, 10 (4), 504-516.

[7] Valíček, J. et al. (2012). Non-contact method for surface roughness measurement after machining. *Measurement Science Review*, 12 (5), 184-188.

[8] Łukianowicz, C., Karpiński, T. (2001). Optical system for measurement of surface form and roughness. *Measurement Science Review*, 1 (1), 151-154.

[9] Xie, Z.X., Zhang, Z.W., Jin, M. (2006). Development of a multi-view laser scanning sensor for reverse engineering. *Measurement Science and Technology*, 17 (8), 2319-2327.

[10] Pettersen, A.D., Rotvold, O., Rotvold, Y. (2000). *Point-by-point measurement system for spatial coordinates - uses opto-electronic cameras, rangefinders, and touch tool having at least three point-shaped light sources, light reflecting points and contact point.* U.S. Patent No. 6,166,809. Washington, D.C.: U.S. Patent and Trademark Office.

[11] Liu, S.G., Huang, F.S., Peng, K. (2005). The modeling of portable 3D vision coordinate measuring system. In *Optical Design and Testig II. Proceedings of SPIE 5638*, 835-842.

[12] Huang, F.S., Qian, H.F. (2009). The model and its solution's uniqueness of a portable 3D vision coordinate measuring system. In *Communications and Photonics Conference and Exhibition (ACP)*, 2-6 November 2009. IEEE, 1-6.

[13] Li, J.J., Zhao, H., Jiang, T., Zhou, X. (2008). Development of a 3D high-precise positioning system based on a planar target and two CCD cameras. In *Intelligent Robotics and Applications. Lecture Notes in Computer Science 5315.* Springer, 475-484.

[14] Zhang, P.W., Zhang, Z.Q., Zhang, Y.F. (2008). The research for a system of binocular stereo vision based on the near-infrared imaging characteristics of black-and-white CCD. In *Infrared Materials, Devices, and Applications. Proceedings of SPIE 6835*, 68351G-1-10.

[15] Mochida, D., Daisaku, M. (2012). *Image measurement machine used for measuring dimension of e.g. semiconductor chip, has fly-eye integrator and lens element comprising inscribed circles whose diameter and focal distance of lens element satisfies preset relationship.* U.S. Patent No. 8,120,844. Washington, D.C.: U.S. Patent and Trademark Office.

[16] Tsai, R.Y. (1987). A versatile camera calibration technique for high-accuracy 3D machine vision metrology using off-the-shelf TV camera and lenses. *IEEE Journal of Robotics and Automation*, 3 (4), 323-344.

[17] Zhang, Z.Y. (2000). A Flexible new technique for camera calibration. *IEEE Transactions on Pattern Analysis and Machine Intelligence*, 22 (11), 1330-1334.

[18] Liu, S.G., Li, P., Na, Y.L. (2002). Evaluation of the form error of ellipse based on least square method. *ACTA Metrological Sinica*, 23 (4), 245-247.

[19] Faugeras, O. (1993). *Three-Dimensional Computer Vision: A Geometric Viewpoint*. The MIT Press, 34-51.

[20] Yuan J.S.-C. (1989). A general photogrammetric method for determining object position and orientation. *IEEE Transactions on Robotics and Automation*, 5 (2), 129-142.

Received October 25, 2012.
Accepted July 29, 2013.